

# **Electrical performance analysis and optimization of monofacial and bifacial crystalline silicon solar cells**

A.V.M. MANIKANDAN\*, SHANTHI PRINCE

Department of ECE, SRM Institute of Science and Technology, Tamilnadu, India

\*Corresponding author: avm.mani@gmail.com

This paper presents the investigations and performance analysis of monofacial and bifacial crystalline silicon solar cells with PC1D simulation software. The fundamental limitation in the monofacial solar cell's performance is its inability to absorb all the incoming solar radiation since the albedo effect (ground-reflected light that can be captured by the rear of the solar cell) is often neglected. So, the efficiency of the monofacial cell will be lower due to poor and incomplete optical absorption. Bifaciality helps to enhance the capturing of light in the solar cell, which means that the rear of the cell is exposed to solar radiation to produce electrical power. The primary focus of our work is to determine which solar cell offers better device performance and conversion efficiency by analyzing various parameters of the solar cell like surface texturing, emitter doping, bulk doping, minority carrier lifetime, bulk and surface recombination rates, front and rear reflectance, among other parameters. The other parameters are maintained at an optimal range to achieve the highest conversion efficiency. Our work has shown that the bifacial solar cell can be as efficient as 28.15%, which is much better than the 22.65% efficiency of the monofacial solar cell.

**Keywords:** silicon, monofacial solar cell, bifacial solar cell, PC1D, quantum efficiency, conversion efficiency, albedo, bifaciality factor, PERT.

## **1. Introduction**

A solar cell is a p-n junction with metal contacts on both sides. They convert solar light directly into electrical power using the electronic properties of semiconductors through the internal photoelectric effect [1]. It is supposed to absorb all the solar radiation falling on it, and it must be designed to maximize the conversion of light to electricity (conversion efficiency). For the solar cell to turn light energy into electrical energy, the primary control process includes making electron-hole pairs, separating charge carriers at the semiconductor junction, and collecting charge carriers. Most semiconductors are good at making electron-hole pairs because they have energy bands or levels

that are separate from each other (defined as the material's band gap). When a photon of sunlight with an energy larger than that of the bandgap strikes the surface of a solar cell, it moves an electron from the lower-energy valence band to the higher -energy conduction band. Because the difference in energy levels in the semiconductor makes the potential energy of electrons go up, this excited electron will stay in the higher energy level for a longer time. This increases the chance of charge separation and, by extension, the power that can be taken from the device [2,3].

In principle, any semiconductor material is suitable for making a solar cell; however, only a few materials can provide a reasonable conversion efficiency. Ideally, the following requirements should be fulfilled by a semiconductor material for suitability as a solar cell material: (i) a bandgap between 1 and 1.5 eV, (ii) an absorption coefficient of  $10^4$  to  $10^6 \text{ cm}^{-1}$ , (iii) a low recombination rate, (iv) a long diffusion length of the generated charge carriers, and (v) materials that are abundant, have reproducible properties and are safe and non-toxic. Several elements satisfy the above requirements, and silicon (Si) is one such, except that it is an indirect bandgap material. The other properties of Si that favour us as the material of our choice for making the solar cell are: abundantly available and can be deposited in several forms as a thin film absorber, such as amorphous Si, microcrystalline Si and polycrystalline Si [4].

There are endless amounts of simulation work in monofacial and bifacial solar cells. A few results have been reported here. ISLAM *et al.* [5] compared the efficiency curves and outputs of a bifacial solar cell and a polycrystalline solar cell. They observed that the bifacial solar cell shows greater efficiency than the polycrystalline solar cell regarding altering cell thickness, emitter doping, and bulk recombination lifetime. They reached the greatest attainable efficiency of a bifacial solar cell at 16.76%, which is more than a polycrystalline solar cell. SEPEAI *et al.* [6,7] used the PC1D simulation program to design and optimize a bifacial solar cell. They also investigated how different parameters impacted the cell, such as emitter doping, bulk doping, minority carrier lifetime, wafer thickness, front and back surface recombination, and illumination from the front and back surfaces. The efficiencies obtained from this design were 16.42% and 14.18% for the front and back surfaces, respectively.

HASHMI *et al.* [8] studied the influence of several solar cell parameters with their implications on power and efficiency. After tweaking the effective parameters, a 20.35% efficient solar cell has been achieved through simulation. THIRUNAVUKKARASU *et al.* [9] reported that a solar cell with a bulk resistivity of  $1 \Omega \cdot \text{cm}$ , a bulk lifetime of 2 ms, an emitter ( $n^+$ ) doping concentration of  $1 \times 10^{20} \text{ cm}^{-3}$  and a shallow back surface field doping concentration of  $1 \times 10^{18} \text{ cm}^{-3}$ , and a surface recombination velocity between  $10^2$  and  $10^3 \text{ cm/s}$  obtained a solar cell efficiency of 19%. AHMED *et al.* [10] have performed a complete simulation of silicon solar cells and evaluated the essential aspects affecting efficiency. They found that the efficiency was impacted by 2.7% through emitter concentration variation, 1.5% through FSRV (front surface recombination velocity), 1% through BSRV (back surface recombination velocity), and 1% through bulk resistivity. The most significant change was recorded for the minority carrier lifetime.

## 2. Design

### 2.1. Device structure

The bifacial solar cell is like a regular solar cell, but its structure is very different. In traditional solar cells, the solar light is made to fall only on the front surface of the cell as its rear side is covered with metal, and hence they produce less electric power. This is where a bifacial differs. It has a symmetric configuration in which the solar light is made to fall on both its surfaces, front and rear. The presence or absence of rear contacts differentiates a monofacial cell from a bifacial cell from a structural standpoint (Fig. 1).

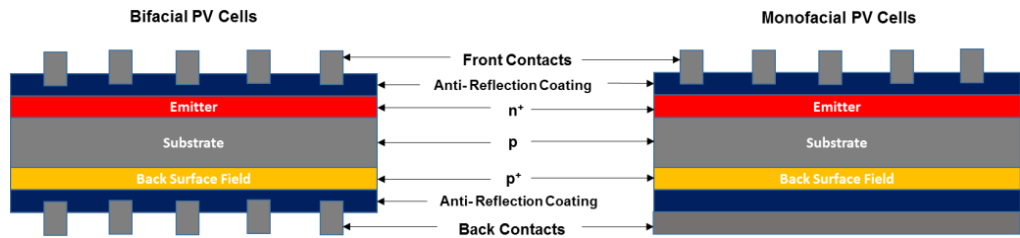


Fig. 1. Typical structure of bifacial and monofacial solar cells.

For monofacial cells, the electrode at the rear side is coated over the whole solar cell's surface, but it is coated in a grid pattern for bifacial cells. This is clear from the illustration, which shows a metallization grid at the rear side of the device that helps absorb radiation from behind, increasing the cell's overall power output. This makes bifacial cells different from monofacial cells, making bifacial cells more efficient than monofacial cells [11-13]. The cell architecture is schematically shown in Fig. 1.

In recent years, the bifacial cell has become more popular because of its many advantageous characteristics, such as (i) a lower working temperature than monofacial cells, which means more power can be made, (ii) fewer recombination losses, which means higher external quantum efficiency, (iii) less degradation from moisture, light, and potential, which means high durability, and (iv) a higher energy density, which means making more energy for the same area. Despite these advantages, the conversion efficiency of the bifacial cell in the wavelength range of 300–500 nm is found to be lower. For this purpose, a heterojunction solar cell can be considered. A heterojunction solar cell is a multi-junction cell made using two dissimilar semiconductor materials. The efficiency of a heterojunction cell stays the same over a wide range of wavelengths, which is a big plus [14].

### 2.2. Simulation setup

Our proposed monofacial and bifacial solar cells are simulated using PC1D, a one-dimensional modelling tool for optical electronics devices. This tool is used not only for the simulation of device performance but also to understand the physics of a solar cell,

especially a silicon solar cell, and to study its electrical and optical parameters [15]. It solves the drift and diffusion, Poisson and continuity equations for each region setup. It has an easy-to-use graphical user interface (GUI) with many input/output parameters for analysis in both space and time domains. It has features to create one's own material parameter files and import exterior reflectance, optical absorption, refractive indices, solar spectrum files, *etc.* It also has library files with the parameters of crystalline semiconductors like Si, Ge, GaAs, AlGaAs, *etc.*, that are used in solar cell technology [5].

The way PC1D works can be broken down into three main steps: first, the user enters the desired vital parameters based on the physical configuration; second, the simulation is run; and third, the user gets the result. To evaluate and compare the efficiency of the two solar cells, a simulation of each cell is run under conditions that are analogous to both cells and with the standard parameters kept unchanged [6]. The typical input parameters for the PC1D tool are listed in Table 1, along with their corresponding values and the units employed throughout the simulation.

The area of a solar cell device chosen is  $10 \times 10 \text{ cm}^2$  (typical value) for both types of solar cells used in this study. The wafer thickness varies between 100 and 400  $\mu\text{m}$ , starting with 100  $\mu\text{m}$  and then varying the wafer thickness to determine the optimum conversion efficiency value of both of the suggested solar cell models, illustrated in Fig. 2.

The choice of material is silicon, and its many default constant values, namely carrier mobility, dielectric constant, bandgap, intrinsic concentration, absorption coefficient and refractive indices, are present in this software. To enhance light absorption or reduce reflection losses, surface texturing is done at the front/rear surface of the solar cell [16]. Surface texturing is the local deviation of a surface from a perfectly flat plane. It allows maximum light to reflect back onto the silicon surface again, rather than being lost to the surrounding air and undergoing multiple reflections [8, 13]. Due to the big

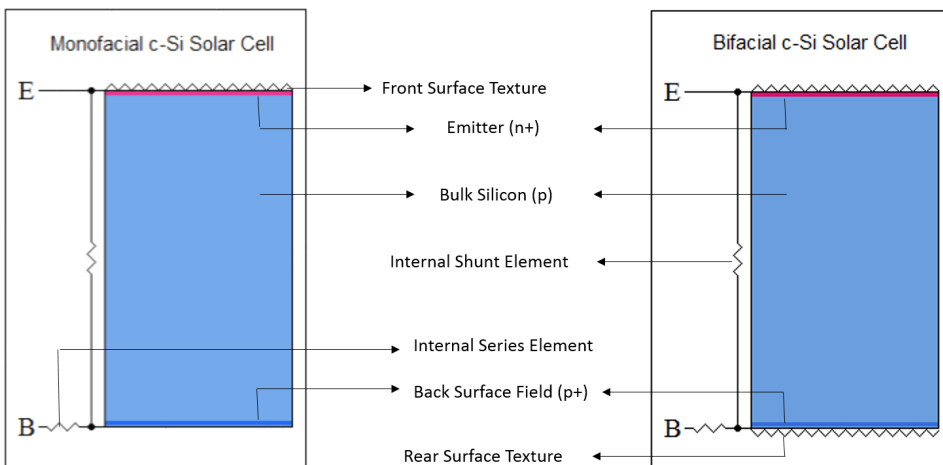


Fig. 2. PC1D model of monofacial and bifacial crystalline silicon solar cells.

difference in index between most semiconductor materials and air, much solar radiation is reflected back from the top of solar cells. Surface texturing depth is the depth of the texturing made on the surface of a solar cell. It can be in the range of 1–4  $\mu\text{m}$ , and the optimum value is chosen as 3  $\mu\text{m}$ . The surface texturing angle is the angle at which the surface needs to be textured, and  $54.74^\circ$  has been selected as the best value. The optimum value is chosen where maximum efficiency is obtained.

Surface texturing, emitter doping, bulk doping, back surface doping, minority carrier lifespan, bulk and surface recombination rates, front and rear reflectance, and illumination from the front and rear surfaces are some essential factors studied in this article. The AM 1.5G spectrum is used in this model, operating under 1 sun condition. All parameters were set to their default values during simulations except those explicitly indicated in Table 1. The optimized process parameters can then serve as the basis for producing solar cells.

Table 1. Simulation parameters.

Parameter	Value and unit
Device	
Device area	100 $\text{cm}^2$
Surface texturing	Front surface textured; angle = $54.74^\circ$ ; depth = 3 $\mu\text{m}$ Rear surface textured; angle = $54.74^\circ$ ; depth = 3 $\mu\text{m}$
Exterior front reflection	2%
Exterior rear reflection	2%
Internal optical reflectance	Enabled; front /rear surface – 10% on first bounce
Emitter contact	Enabled; internal series resistance = $1 \times 10^{-6} \Omega$
Base contact	Enabled; internal series resistance = 1 $\text{m}\Omega$
Internal shunt elements	Enabled; conductance = 0.33 S
Region-1	Base/Substrate
Thickness	200 $\mu\text{m}$
Material	Si
Background doping	P-type; $1 \times 10^{16} \text{ cm}^{-3}$
Front diffusion	N-type; $1 \times 10^{18} \text{ cm}^{-3}$
Rear diffusion	P-type; $1 \times 10^{19} \text{ cm}^{-3}$
Bulk recombination	$\tau_n = \tau_p = 1000 \mu\text{s}$
Front-surface recombination	$S_n = 100 \text{ cm/s}$ ; $S_p = 0 \text{ cm/s}$
Rear-surface recombination	$S_n = 0 \text{ cm/s}$ ; $S_p = 100 \text{ cm/s}$
Excitation	
Temperature	$25^\circ\text{C}$
Base circuit	–0.7 to 0.7'
Light source	Front/rear
Light intensity	Primary light source enabled: constant intensity of 0.1 $\text{W/cm}^2$ Sec. light source enabled: constant intensity of 0.033 $\text{W/cm}^2$
Spectrum	AM 1.5G

### 3. Results and discussion

#### 3.1. The impact of wafer thickness on solar cell efficiency

For a solar cell to convert light into electricity as efficiently as possible, the active layer must be optically thick (so it can absorb as much incident radiation as possible) and electronically thick (to reduce surface recombination and maximize carrier collection efficiency). So, for a given quality of material, the best thickness of the active layer is a balance between high optical absorption and good carrier collection. Here, we examine how the computed figures of merit (conversion efficiency, short-circuit current, open-circuit voltage, and fill factor) change with the thickness of the material.

The wafer thickness of each solar cell varied from 100 to 400  $\mu\text{m}$ , while the other parameters of the solar cell were kept constant (as shown in Table 1). This was done to see how the short-circuit current density ( $J_{\text{SC}}$ ), open-circuit voltage ( $V_{\text{OC}}$ ), fill factor (FF), and conversion efficiency ( $\eta$ ) changed for each solar cell. Figure 3 illustrates how these electrical parameters change as the thickness changes.

As can be seen in Fig. 3, the efficiency of a monofacial solar cell increases rapidly up to a thickness of about 200  $\mu\text{m}$  and then drops at an even more, slower rate. With a thickness of 400  $\mu\text{m}$ , monofacial c-Si solar cells achieve an efficiency of 22.81%.

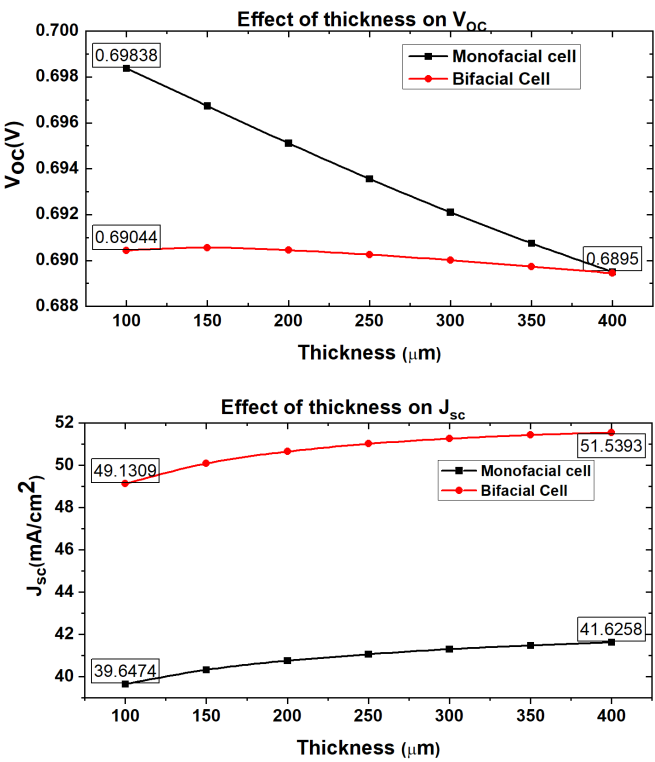


Fig. 3. Solar cell electrical parameters vs. wafer thickness.

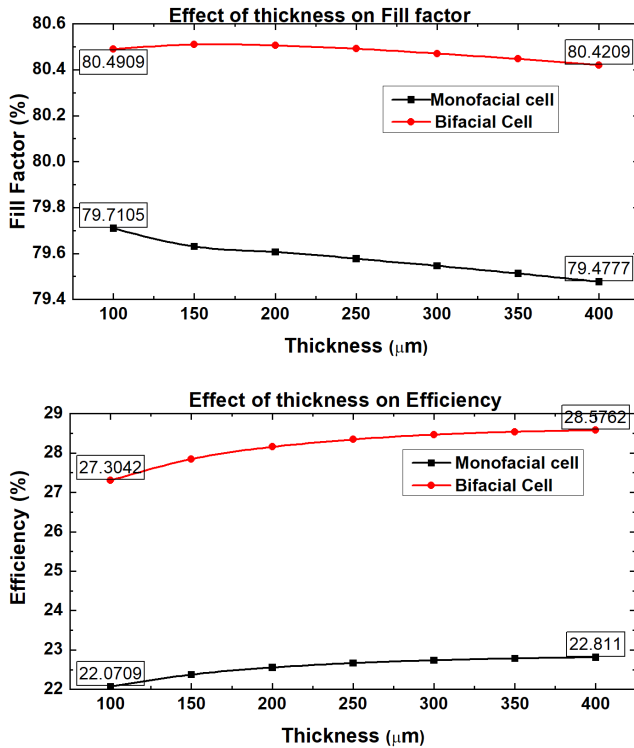


Fig. 3. Continued.

The efficiency curve of bifacial solar cells is very similar to that of monofacial cells. However, on average, bifacial cells are 5.6% more efficient than monofacial cells. At 400  $\mu\text{m}$  in thickness, the efficiency hits 28.58%. In both cells, the rate at which efficiency increase slows down past 200  $\mu\text{m}$ . As a result, the optimal thickness, yielding the highest efficiency from both cells, is determined to be 200  $\mu\text{m}$ . Using the optimal wafer thickness will help cut down on the cost of materials [5,9,17,18].

### 3.2. The impact of emitter doping on solar cell efficiency

The formation of the p-n junctions through diffusion is a crucial stage in manufacturing solar cells. There are two forms of diffusion in a solar cell: front and back. Front diffusion refers to the diffusion that occurs at the front surface. Since electron mobility is great and they diffuse quickly into the surface, the front diffusion is *n*-type [5,6,9,18,19]. Concentrations of doping levels are crucial to the functioning of a solar cell. Keeping all other parameters constant, we altered the emitter doping levels of each solar cell from  $10^{17}$  to  $10^{20} \text{ cm}^{-3}$  and studied their impacts on efficiencies.

Figure 4 illustrates the impact of the emitter doping level on the efficiency of both solar cells under consideration. It demonstrates that the efficiency of monofacial solar cells is constant and maximal at approximately 22.4% when the emitter doping level

is  $10^{19} \text{ cm}^{-3}$ ; after that, the efficiency declines substantially. Also, we may observe that the bifacial solar cell functions virtually identically until the doping concentration reaches  $10^{19} \text{ cm}^{-3}$ , at which point it reaches a maximum efficiency of 22.92%, after which it declines drastically. The optimal emitter doping level is carefully chosen to be neither too low nor too high. A low doping profile increases the sheet resistance, which in turn lowers the efficiency of the conversion. On the other hand, a strong dop-

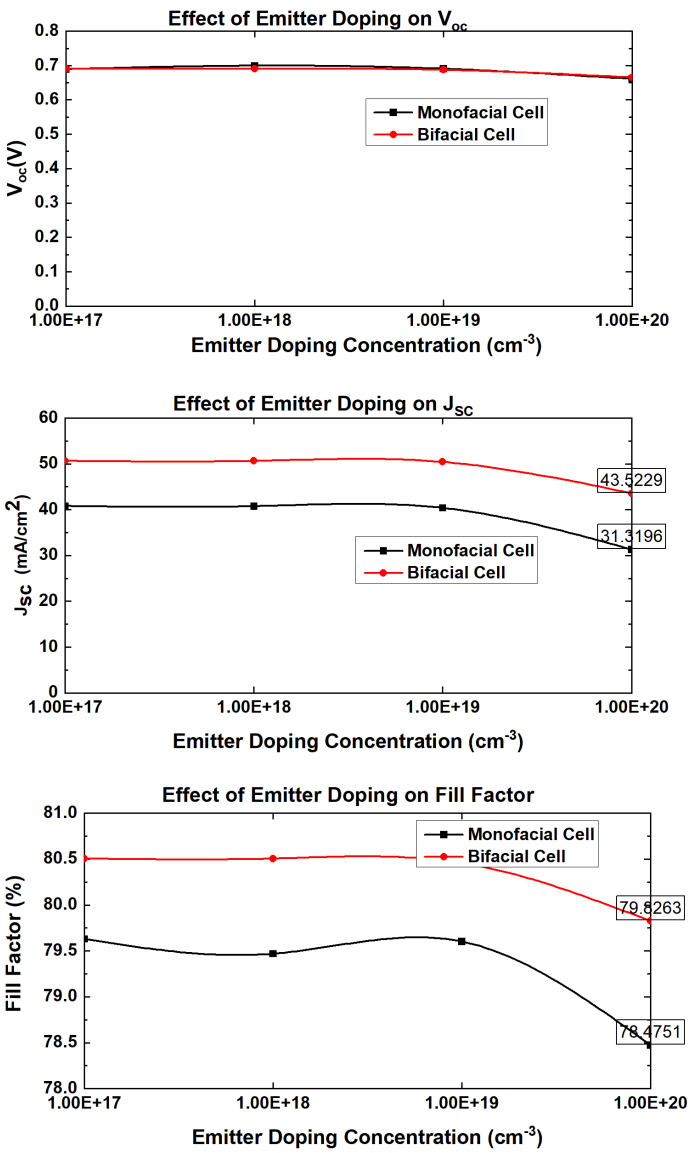


Fig. 4. Solar cell electrical parameters vs. emitter doping.



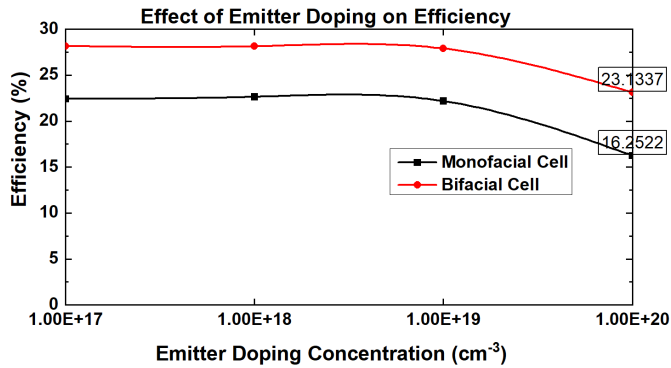


Fig. 4. Continued.

ing profile results in significant carrier recombination losses, making solar cells less efficient. Taking these factors into account, the best emitter doping level for both solar cells is found to be  $10^{19} \text{ cm}^{-3}$ . We can figure out that other electrical parameters of the solar cell, such as  $J_{SC}$ ,  $V_{OC}$  and FF, follow similar trends.

### 3.3. The impact of back surface field (BSF) doping on solar cell efficiency

Back surface field (BSF) refers to the heavily doped layer on the rear of the solar cell. The boundary between a solar cell's deep and shallow doped regions creates an electric field at the BSF's interface, just like a p-n junction. They function as a barrier for minority carrier passage towards the rear surface, reducing rear surface recombination [6, 9, 10, 18, 19]. By holding the  $n^+$  emitter's doping at  $1 \times 10^{18} \text{ cm}^{-3}$ , the BSF doping level was changed from  $10^{17}$  to  $10^{22} \text{ cm}^{-3}$ . The variation in the current-voltage parameters of the solar cell with BSF doping level is depicted in Fig. 5.

The best-reported efficiency was achieved with a solar cell whose doping concentration was  $1 \times 10^{19} \text{ cm}^{-3}$ ; hence, this value was selected as the optimal doping con-

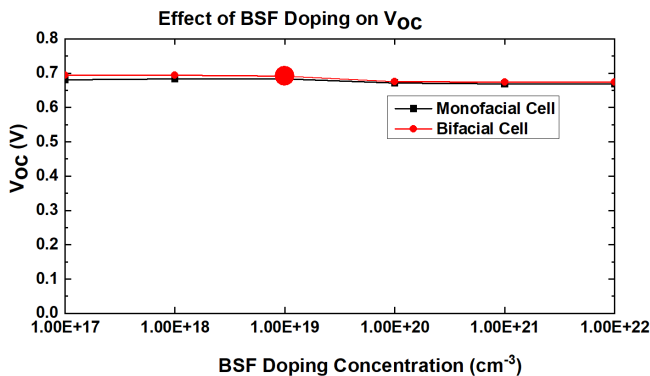


Fig. 5. Solar cell electrical parameters vs. BSF doping.

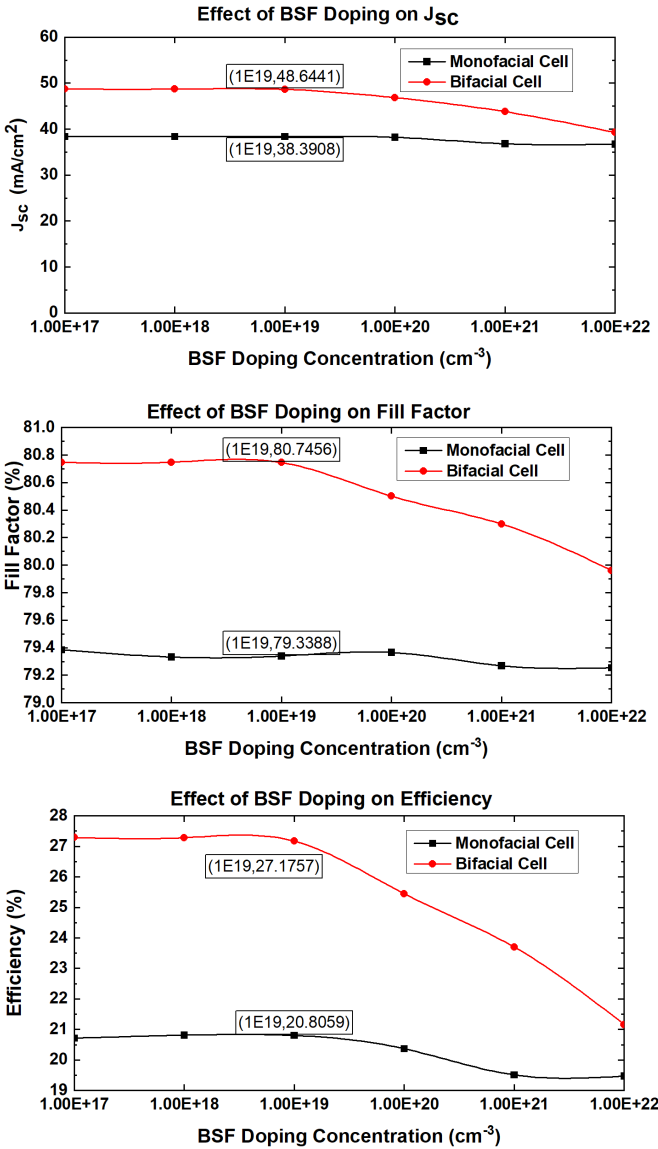


Fig. 5. Continued.

centration for the BSF layer. The amount of BSF doping significantly affects the device's other I-V parameters. The I-V parameters saturate until the doping level reaches  $1 \times 10^{19} \text{ cm}^{-3}$ , but beyond that, the I-V parameters gradually decline, and cell performance rapidly diminishes with increasing doping concentrations. This is due to the increase in  $R_{\text{sheet}}$ , which causes an increase in contact resistance, resulting in a drop in the cell's  $V_{\text{OC}}$  and  $J_{\text{SC}}$ .

### 3.4. The impact of bulk doping on solar cell efficiency

In this study, the  $n^+$  emitter and  $p^+$  BSF doping concentrations were maintained at  $1 \times 10^{19} \text{ cm}^{-3}$  for modelling purposes. The bulk doping concentration (background doping) was changed from  $1 \times 10^{13}$  to  $1 \times 10^{17} \text{ cm}^{-3}$ , and the cell's I-V parameters were

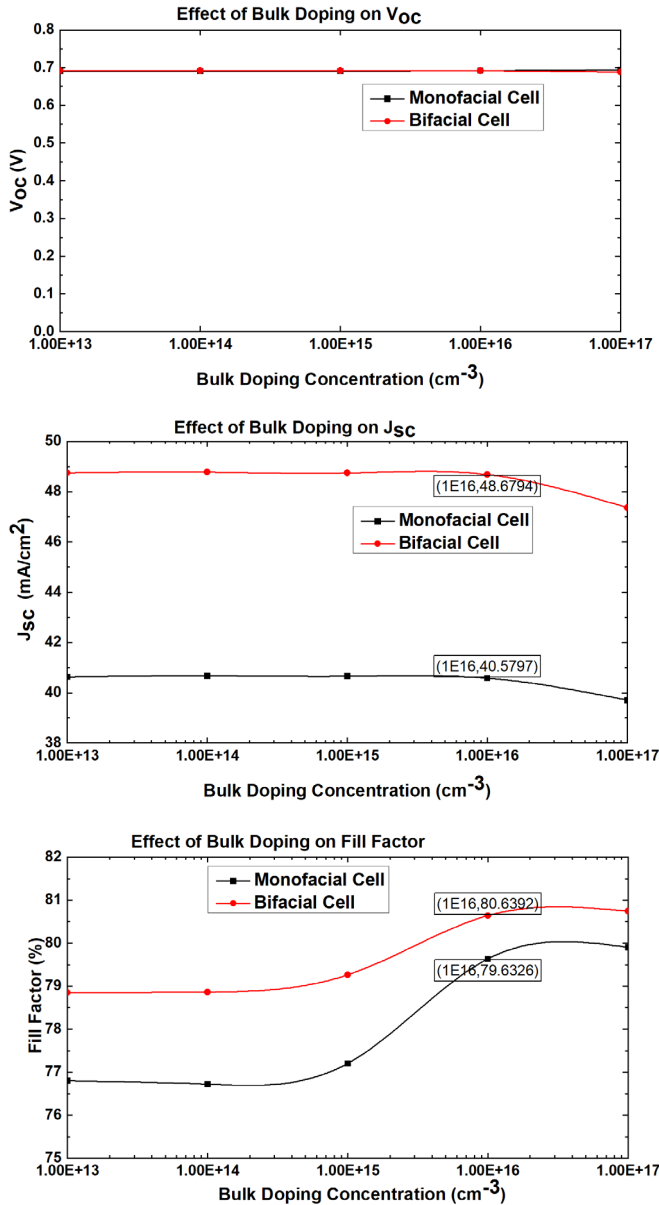


Fig. 6. Solar cell electrical parameters vs. bulk doping.

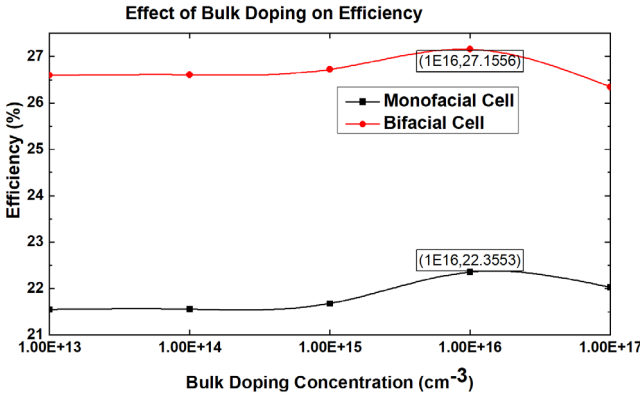


Fig. 6. Continued.

measured. Figure 6 shows how the I-V parameters of a cell change as the bulk doping concentration changes. For monofacial cells, the maximum efficiency was achieved at a doping concentration of  $1 \times 10^{16} \text{ cm}^{-3}$ , while the efficiency rapidly decreased for bulk doping levels of  $1 \times 10^{17} \text{ cm}^{-3}$  and above. Similar behaviour can be seen with bifacial c-Si solar cells.

The minority carrier lifetime gets shorter as the amount of bulk doping goes up. It has been found that there isn't much radiative recombination when the bulk doping density is less than  $10^{17} \text{ cm}^{-3}$ . But Auger recombination is more likely to happen when the bulk doping is more than  $10^{18} \text{ cm}^{-3}$  [8,9]. The same justification applies to the requirement that the bulk doping levels be lower than the diffusion doping levels. Background doping is best set at a value of  $1 \times 10^{16} \text{ cm}^{-3}$ .

### 3.5. The impact of bulk resistivity on solar cell efficiency

Bulk resistivity is an important performance metric for solar cells, and it is determined by the bulk material's doping density. Bulk resistivity has a more intricate relationship

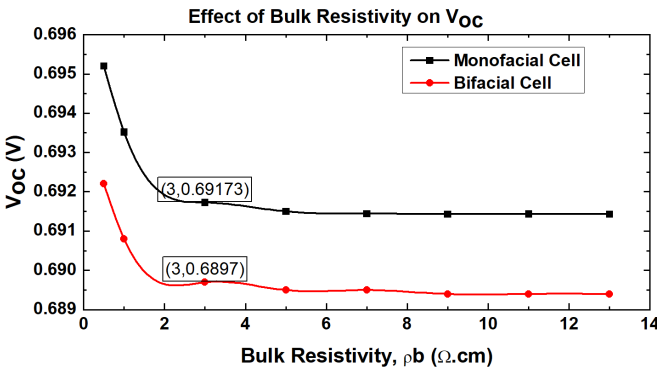


Fig. 7. Solar cell electrical parameters vs. bulk resistivity.

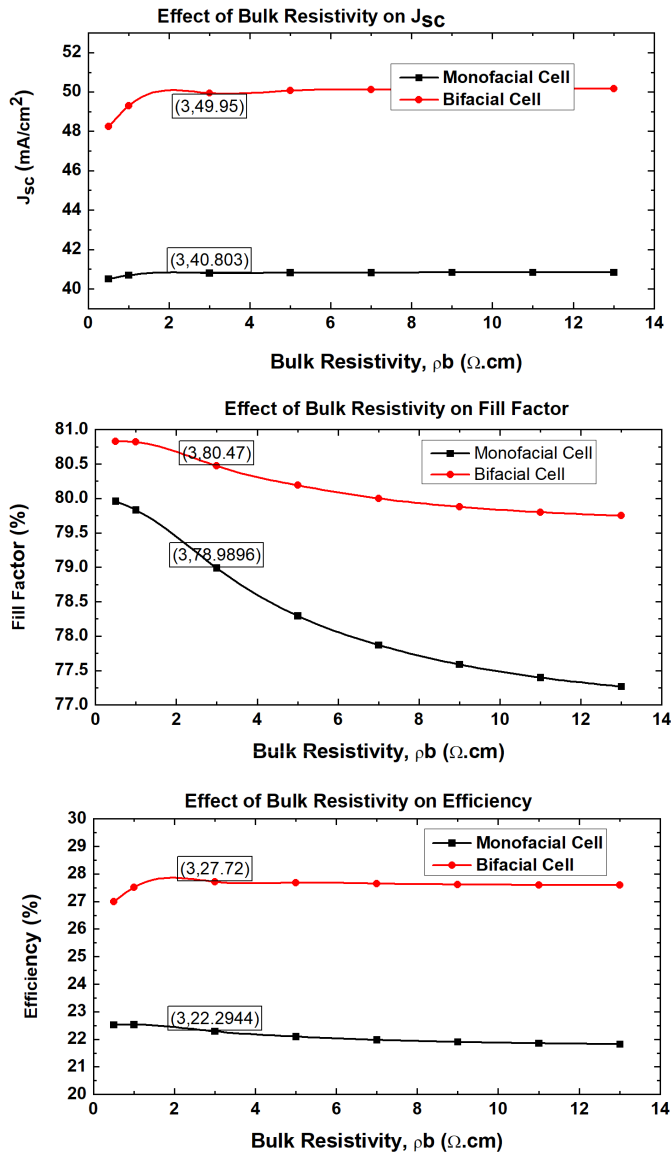


Fig. 7. Continued.

to the I-V behaviour of a solar cell than the other parameters. Bulk resistivity directly influences the conversion efficiency of the solar cell due to its effect on the carrier profile across the cell, the mobility of charge carriers, the bulk recombination current, and as well the lifetime of carriers [20]. When the shunting channel runs through the base, the bulk resistivity also impacts the internal resistance, particularly the shunt resistance.  $J_{SC}$  increases,  $V_{OC}$  lowers, and FF generally reduces when bulk resistivity rises. The resistivity of a wafer can be modulated based on the bulk doping levels (Fig. 7).

In making silicon solar cells, the change in wafer resistivity and its effect on efficiency makes it a fascinating topic to investigate [21].

Industrial production currently uses single-crystalline silicon wafers of p-type with a resistivity between and including  $0.5\text{--}2\ \Omega\cdot\text{cm}$ . The calculated figures show that a c-Si wafer doped to a level of  $10^{15}$  to  $10^{16}\ \text{cm}^{-3}$  can produce a wafer resistivity in the range of  $1$  to  $10\ \Omega\cdot\text{cm}$ , making it suitable for use in the manufacturing of solar cell devices. Recombination losses may increase if we select a wafer with a lower resistivity (less than  $1\ \Omega\cdot\text{cm}$ ) since a lower resistivity correlate to an increased doping intensity. This may result in decreased  $J_{\text{SC}}$  and conversion efficiency [10].

### 3.6. The impact of bulk recombination lifetime on solar cell efficiency

Holes and electrons excited by light absorption also suffer from a loss mechanism. If an excited electron and hole meet each other, they can recombine. They join each other and lose their mobility, *i.e.*, the electrons are glued again to the background in a molecular orbital [7]. There are two types of recombination: bulk and surface recombination. Electron–hole recombination occurring at the bulk of the substrate (*i.e.*, in its portion away from the surface) is known as bulk recombination [5,9,17]. The bulk re-

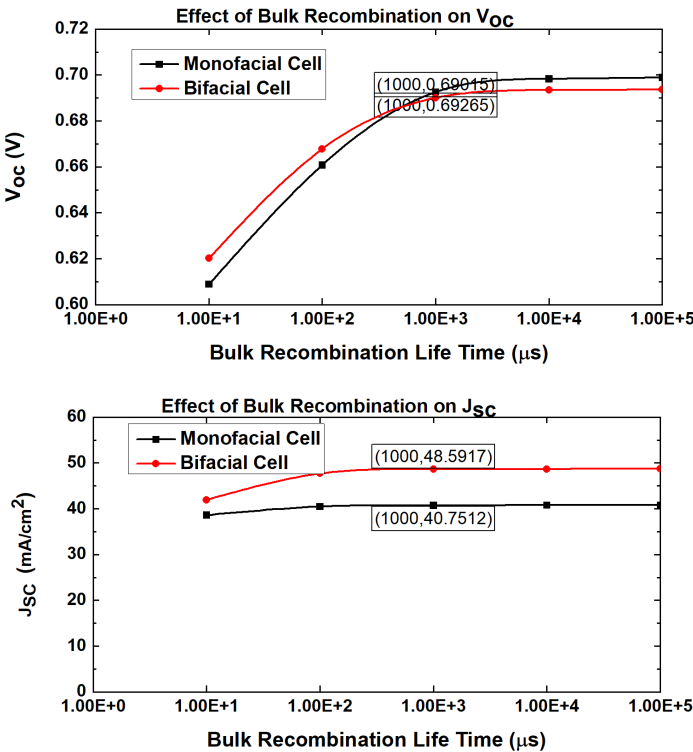


Fig. 8. Variation in  $V_{\text{OC}}$ ,  $J_{\text{SC}}$ , FF and efficiency as a function of bulk recombination lifetime.

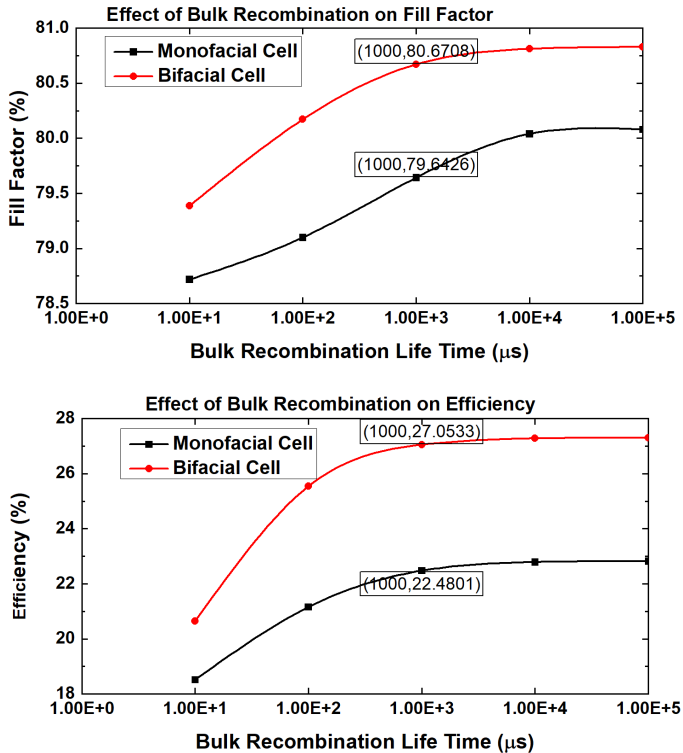


Fig. 8. Continued.

combination involves the carrier lifetimes to be mentioned. High-lifetime wafers show better solar cell efficiencies than low-lifetime wafers for both solar cells (Fig. 8).

The optimum value of carrier lifetime for the simulation of both solar cells is  $1000 \mu\text{s}$ , the value below which the I-V parameters of the solar cell decrease and above which the I-V parameters become maximum and constant.

### 3.7. The impact of surface recombination velocity on solar cell efficiency

Surface recombination refers to the electron–hole recombination in a semiconductor through electrically active centres (defects) at its surface. Surface recombination velocity (SRV) is the speed at which the charge carriers recombine at the surface of a silicon solar cell. If the recombination rate is high at the surface vicinity, the region will be depleted of minority charge carriers. This density gradient causes diffusion of charge carriers resulting in a net movement of charge carriers from the region of higher concentration (surrounding zones) to the region of lower concentration (surface vicinity). The diffusion rate of these minority carriers determines the surface recombination rate and hence the SRV, which is expressed in units of  $\text{cm/s}$ . A high SRV at the emitter front surface will cause charge carrier losses and, as a result, a low short-circuit cur-

rent [22]. Figure 9 depicts the solar cell electrical parameters variation to the front surface recombination velocity (FSRV) and back surface recombination velocity (BSRV).

In the first scenario, the FSRV was changed from  $10^1$  to  $10^6$  cm/s by setting the BSRV at  $10^4$  cm/s. In this simulation, the minority carrier lifetime of the p-type silicon wafer was chosen as  $1000\text{ }\mu\text{s}$  for convenience. In both cells, the I-V parameters  $V_{OC}$ ,  $J_{SC}$ , FF, and  $\eta$  reach their maximum values until  $FSRV = 10^3$  cm/s. These characteristics degrade when FSRV exceeds  $10^3$  cm/s. Simulation results indicate that wafers

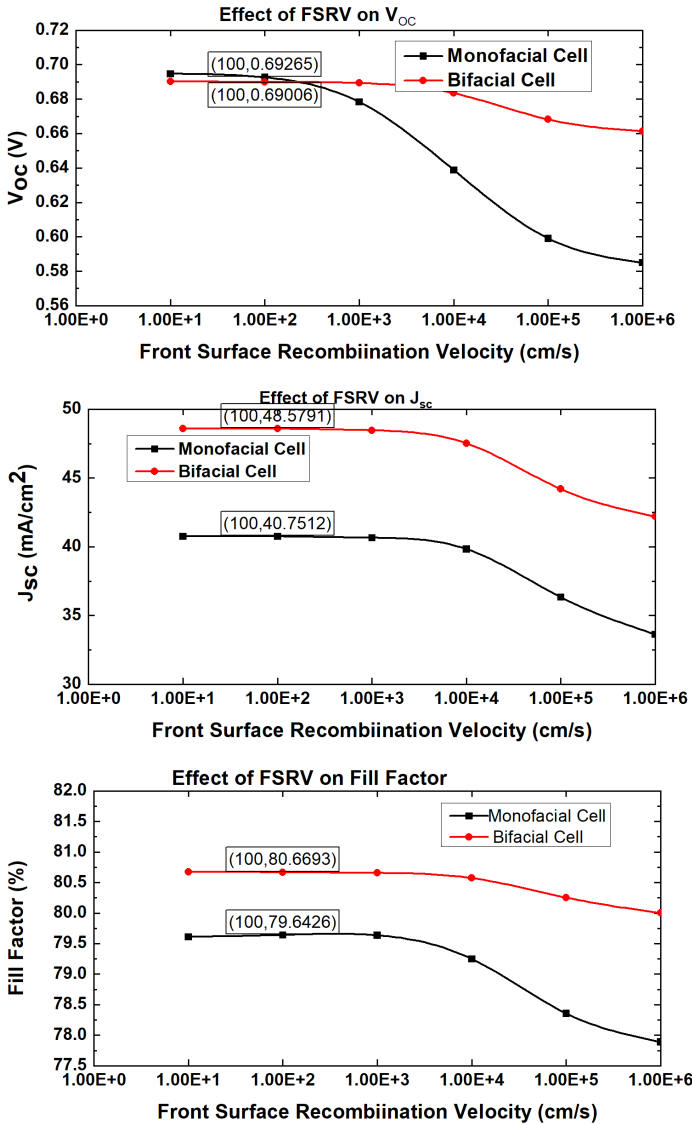


Fig. 9. Solar cell electrical parameters vs. FSRV.



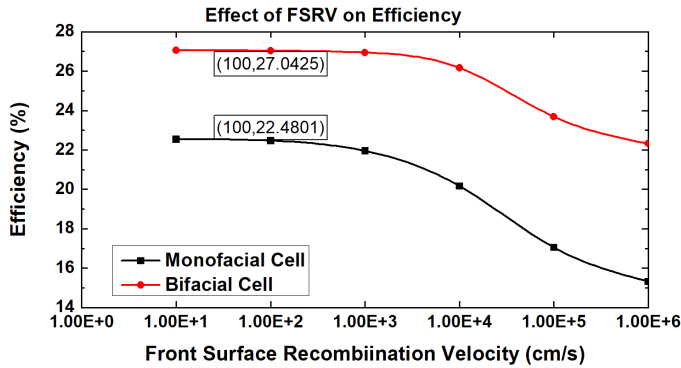


Fig. 9. Continued.

with a high minority carrier lifetime can achieve higher efficiencies with FSRV values between  $10^2$  and  $10^3$  cm/s. The higher the FSRV, the faster the recombination and, as a result, the poorer the efficiency. In the second scenario, the BSRV was varied between  $10^1$  and  $10^6$  cm/s by setting the FSRV at  $10^4$  cm/s (see Fig. 10). This is done to learn how BSRV affects solar cell efficiency. The simulation shows that changing the BSRV

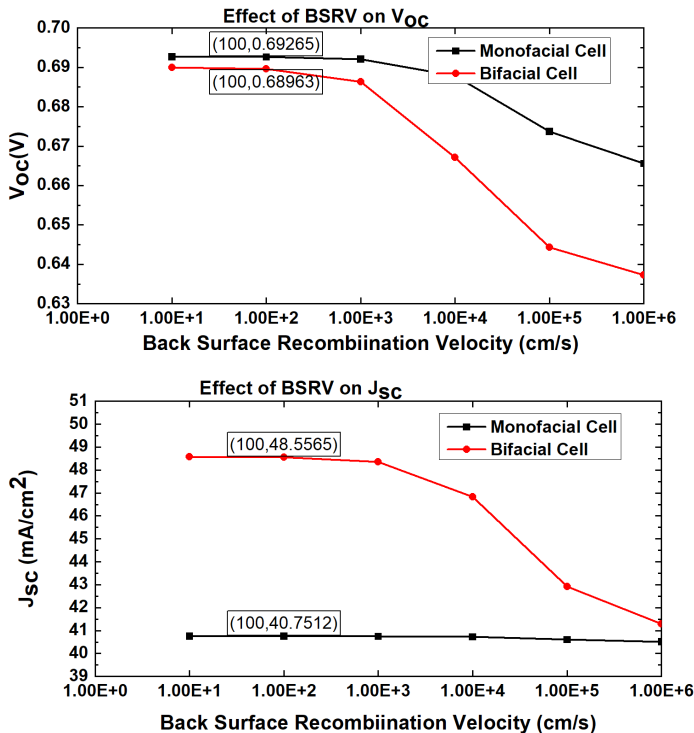


Fig. 10. Solar cell electrical parameters vs. BSRV.

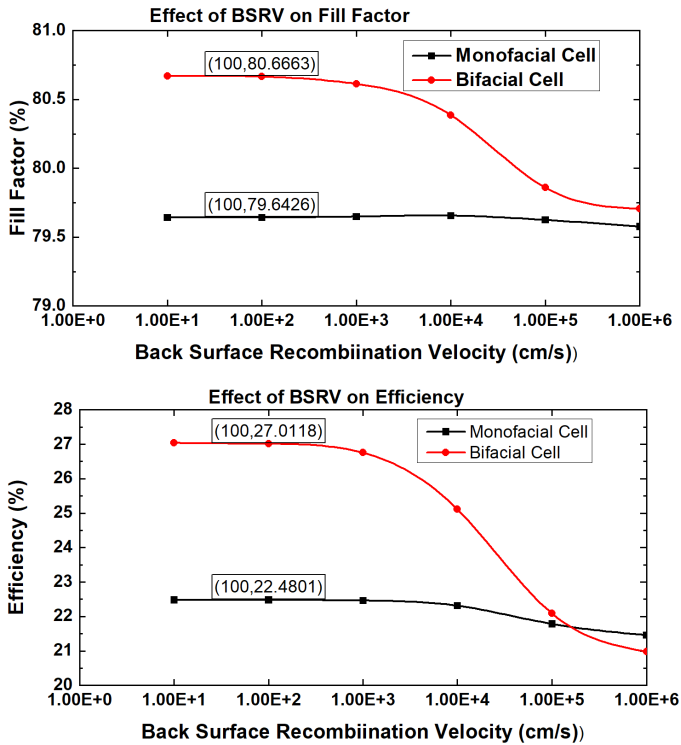


Fig. 10. Continued.

considerably impacts the rear surface contact. In thin wafers, this effect is more prominent. The BSRV should be between  $10^2$  and  $10^3$  cm/s to ensure excellent efficiency.

Two techniques can reduce surface recombination: (i) by lowering the number of surface imperfections in the c-Si. This is accomplished by depositing a thin layer, called the passivation layer, of another material on top of the emitter layer of the solar cell. This layer needs to be an insulator so that electrons are forced to remain within the emitter layer and move through it [9]. Examples include silicon oxide silicon nitride or a stack of aluminium oxide and titanium oxide layers. The bonding environment of the Si atoms is partially restored by these layers. (ii) By lowering the minority carrier density near the surface. This can be accomplished by increasing the emitter layer's doping.

When the recombination occurs at the rear surface of a solar cell, it is called "rear surface recombination". The best way to cut down on rear surface recombination is to use heavily doped point contacts and thermal oxide layers. The thermal oxide layer is a passivation layer for the non-contact area to minimize undesirable surface recombination. The interface between the heavily doped and lightly doped regions acts as a BSF, making it hard for minority charge carriers to move around. Thus, the BSF provides a net effect of passivation at the rear surface. The optimum back surface recombination velocity value is 100 cm/s.

### 3.8. The impact of internal resistances on solar cell efficiency

Solar cells possess internal resistances ( $R_{\text{series}}$  and  $R_{\text{shunt}}$ ), the parasitic elements representing losses in the device. Although internal resistances do not affect the cell's  $V_{\text{OC}}$  and  $J_{\text{SC}}$ , they reduce the cell's fill factor and conversion efficiency [23]. This is illustrated in Figs. 11 and 12. Simulations show that  $R_{\text{series}}$  and  $R_{\text{shunt}}$  significantly affect the solar cell's fill factor and conversion efficiency, but they do not have much of an impact on the other electrical parameters for both monofacial and bifacial c-Si solar

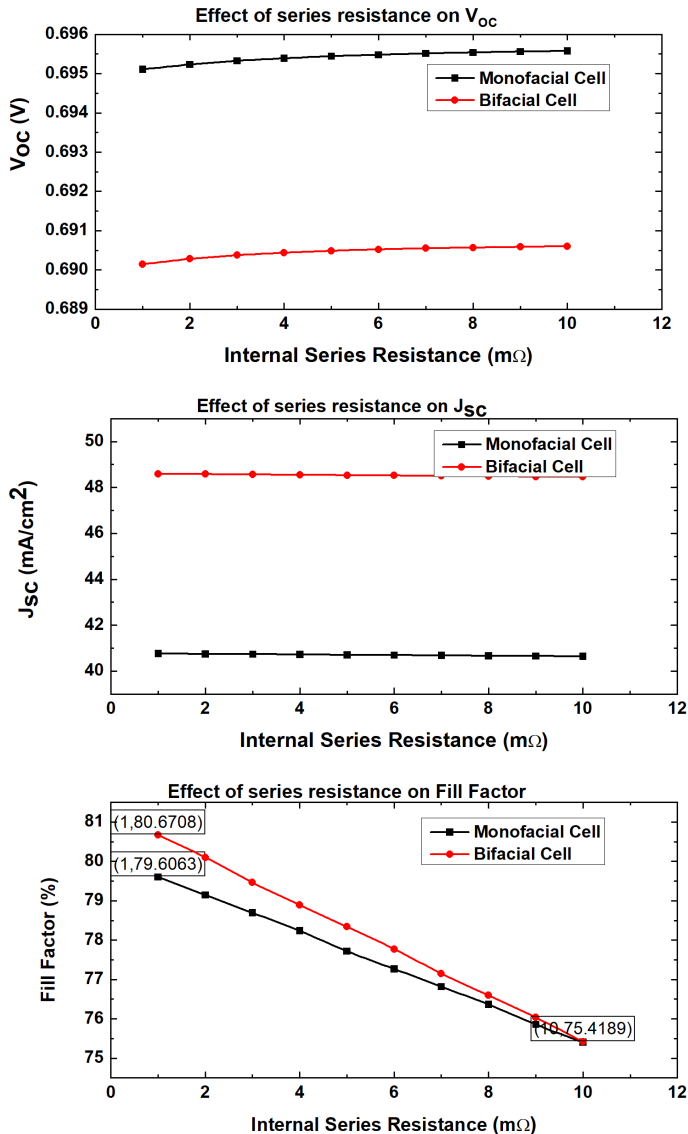


Fig. 11. Solar cell electrical parameters vs.  $R_{\text{series}}$ .

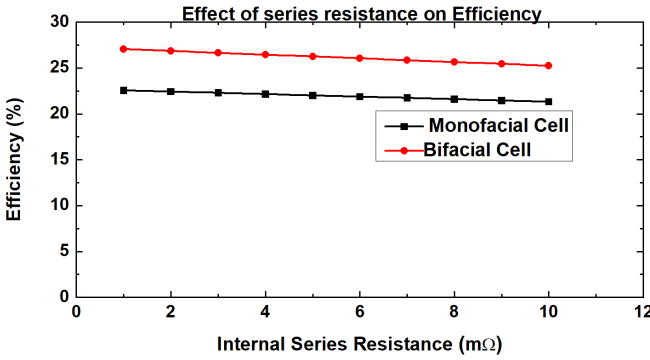


Fig. 11. Continued.

cells. Significant fill factor losses occur when  $R_{shunt}$  is insufficiently high and  $R_{series}$  is insufficiently low.  $R_{series}$  is caused by dangling silicon bonds that form at the cleavage.  $R_{shunt}$ , on the other hand, is usually caused by manufacturing defects rather than poorly designed solar cells. Passivating the surface of the silicon substrate using the passivation layers can overcome the loss mechanisms and thereby obtain better performance of the solar cells [10].

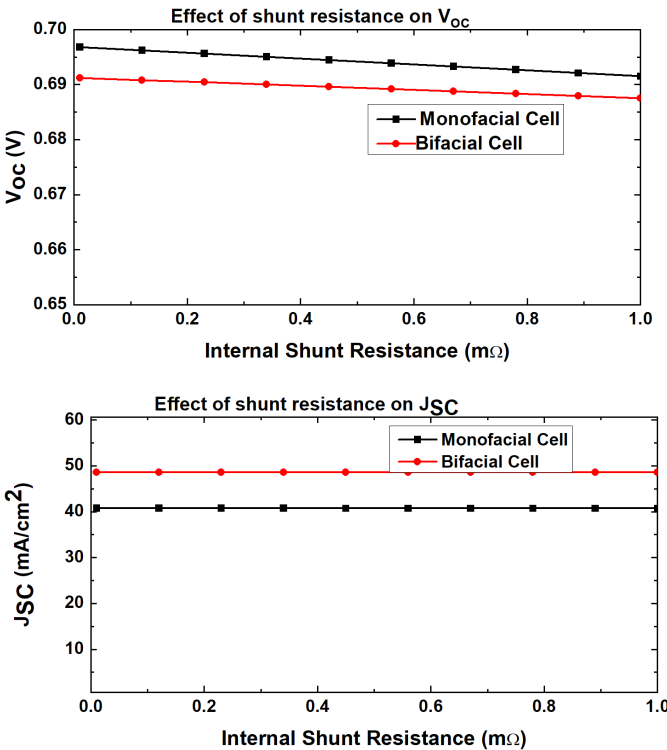


Fig. 12. Solar cell electrical parameters vs.  $R_{shunt}$ .

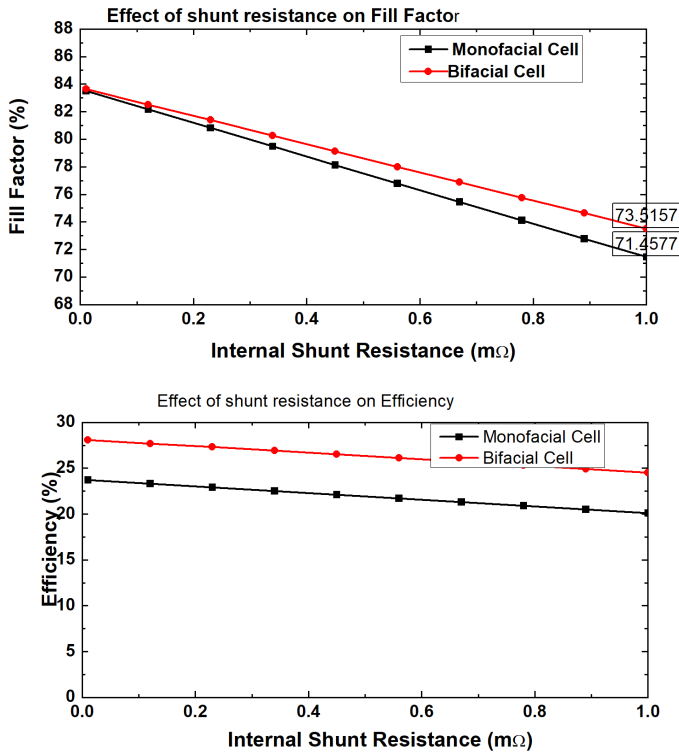


Fig. 12. Continued.

### 3.9. I-V curves

Figures 13(a) and (b) show a typical light current-voltage (I-V) measurement of monofacial and bifacial (under different albedo conditions) solar cells under  $0.1 \text{ W/cm}^2$  light

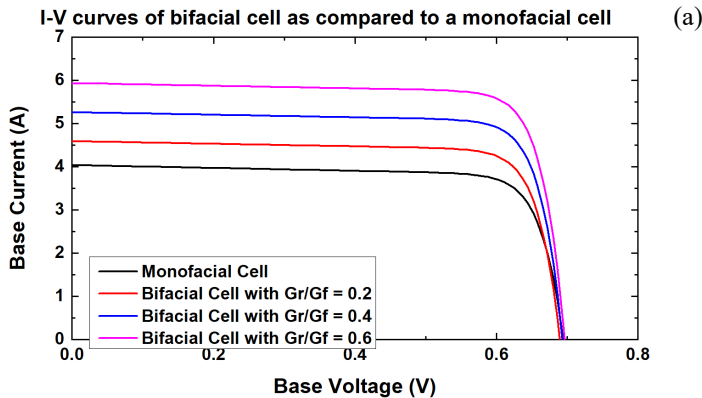


Fig. 13. I-V curves of (a) monofacial cell compared to bifacial cell with different albedo factors, and (b) bifacial cell with single-side illumination.

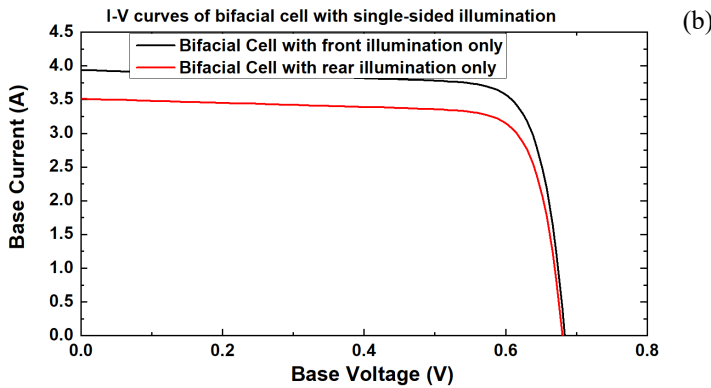


Fig. 13. Continued.

illumination. The plot shows that better I-V characteristics are obtained for bifacial cells with a higher albedo than for those with a lower albedo. Based on these results, we can say that a bifacial PV cell will yield greater gains as albedo increases. The  $V_{OC}$  obtained from the device was around 680–690 mV for both monofacial and bifacial cells (under single-side and simultaneous illumination). The  $J_{SC}$  is higher for bifacial cells (increasing with the albedo factor) than for the monofacial cell. In general, the rear surface current density of the bifacial solar cell used for research in this work was approximately two-thirds of the current density from the front surface.

Table 2 shows a device performance comparison between p-type crystalline silicon passivated emitter and rear totally-diffused (PERT) monofacial and bifacial solar cells. These measurements were made while keeping both cells in optimal and similar conditions. A simulation was run to explore the potential of bifacial p-PERT solar cells to generate power when compared to their monofacial counterparts. The results demonstrate that bifacial solar cells generate more  $J_{SC}$  and power than monofacial cells.

T a b l e 2. Performance comparison between c-Si PERT monofacial and bifacial solar cells.

Cell type	$J_{SC}$ [mA/cm <sup>2</sup> ]	$V_{OC}$ [V]	FF [%]	$P_{max}$ [mW/cm <sup>2</sup> ]	Efficiency [%]
Monofacial	40.76	0.6951	79.61	22.56	22.56
Bifacial (front illumination only)	38.93	0.6836	79.87	21.25	21.25
Bifacial (rear illumination only)	34.27	0.6774	79.41	18.43	18.43
Bifacial (simultaneous illumination with albedo = 0.2)	46.14	0.6867	80.39	25.47	25.47
Bifacial (simultaneous illumination with albedo = 0.3)	49.57	0.6884	80.61	27.51	27.51
Bifacial (simultaneous illumination with albedo = 0.4)	53	0.6901	80.78	29.55	29.55
Bifacial (simultaneous illumination with albedo = 0.6)	59.86	0.6934	81.04	33.64	33.64

## 4. Conclusion

This paper presents a comparative investigation of the effects of the most significant parameters of monofacial and bifacial solar cells. Even though the simulations of these two cells were done under the same conditions in PC1D software, we found that the bifacial solar cell performed better and converted power more efficiently than the monofacial solar cell. Much research was done on the absorber layer, the emitter layer, and the back surface field layer, focusing on the levels of doping, the thicknesses, and how carriers recombine. Research and results show that the best way to design and make a highly efficient PV cell is to know and predict the effects of these critical electrical parameters and use simulation to estimate their optimal values.

The results showed that a single-crystalline silicon wafer of p-type with a resistivity of  $3\ \Omega\cdot\text{cm}$  and a thickness of  $200\ \mu\text{m}$ , with an  $n^+$  emitter BSF doping intensity of  $1 \times 10^{18}\ \text{cm}^{-3}$  and a  $p^+$  emitter BSF doping intensity of  $1 \times 10^{19}\ \text{cm}^{-3}$ , can give a bifacial solar cell efficiency of 28.15%. Maximum efficiency can only be achieved with FSRV and BSRV between  $10^2$  and  $10^3\ \text{cm/s}$ . Minority carrier lifetime, on the other hand, cannot be controlled because it depends on the wafer that was used to make the chip. Single crystalline Si wafers used in fabrication are thought to have a lifetime of only  $5\ \mu\text{s}$ . Instead, a  $1000\ \mu\text{s}$  lifespan has been employed in the simulated case, leading to excellent performance for both surfaces of the bifacial solar cell. In future research, the optimized process parameters will be used to make a working solar cell device that can be used to compare practical and theoretical results.

## Declarations

**Ethics approval:** This is the authors' original work, which has not previously been published elsewhere. The paper is not being considered for publication elsewhere at the moment. The article wholly and accurately reflects the author's own research and analysis.

**Conflict of interest:** The authors declare that they do not have any potential conflicts of interest regarding this article's research, authorship, and/or publication.

**Research involving Human Participants and/or Animals:** This article contains no studies involving animals or human subjects conducted by any authors.

**Consent to participate:** As there are no human subjects in this study, formal consent is not required.

**Consent for publication:** All named authors have read the manuscript and approved it for submission.

**Availability of data and materials:** Data sharing doesn't apply to this article because no datasets were made or analyzed during this study.

**Competing interests:** The authors have no relevant financial or non-financial interests to disclose.

**Funding:** The authors declare that no funds, grants, or other support were received during this article's research and/or preparation that could have influenced its outcome.

### Authors' contributions:

Manikandan AVM: He carried out the design and simulation, examined and analyzed the data, created the figures and graphs, and composed the manuscript as the first author.

Shanthi Prince: As Manikandan AVM's supervisor, she initiated the research, helped with the modelling, suggested creative ideas, and developed and revised the work critically for key intellectual aspects.

### Acknowledgements

The authors thank the SRM Institute of Science and Technology in Chennai, India, for their assistance and facilities in carrying out this research.

### References

- [1] GRAY J.L., [In] *Handbook of Photovoltaic Science and Engineering*, [Eds.] Luque A., Hegedus S., Second Ed., John Wiley & Sons, 2010: 82-129. <https://doi.org/10.1002/9780470974704.fmatter>
- [2] MEHMOOD H., NASSER H., TAUQEER T., TURAN R., *Numerical analysis of dopant-free asymmetric silicon heterostructure solar cell with SiO<sub>2</sub> as passivation layer*, International Journal of Energy Research **44**(13), 2020: 10739-10753. <https://doi.org/10.1002/er.5720>
- [3] KITAI A., *Principles of Solar Cells, LEDs and Diodes: The role of the PN junction*, First Ed., John Wiley & Sons, 2011. <https://doi.org/10.1002/9781119974543>
- [4] BECKER C., AMKREUTZ D., SONTHEIMER T., PREIDEL V., LOCKAU D., HASCHKE J., JOGSCHIES L., KLIMM C., MERKEL J.J., PLOCICA P., STEFFENS S., RECH B., *Polycrystalline silicon thin-film solar cells: Status and perspectives*, Solar Energy Materials and Solar Cells **119**, 2013: 112-123. <https://doi.org/10.1016/j.solmat.2013.05.043>
- [5] ISLAM R., ABRAR M.M., *Comparative analysis of a bifacial and a polycrystalline solar cell device performances by optimizing effective parameters using PC1D*, [In] *2020 International Conference on Smart Grid and Clean Energy Technologies (ICSGCE)*, 2020: 16-20. <https://doi.org/10.1109/ICSGCE49177.2020.9275602>
- [6] SEPEAI S., ZAIDI S.H., DESA M.K.M., SULAIMAN M.Y., LUDIN N.A., ADIB IBRAHIM M., SOPIAN K., *Design optimization of bifacial solar cell by PC1D simulation*, Journal of Energy Technologies and Policy **3**(5), 2013: 1-11.
- [7] SEPEAI S., CHEOW S.L., SULAIMAN M.Y., SOPIAN K., ZAIDI S.H., *Fabrication and characterization of Al-BSF bifacial solar cell*, [In] *2013 IEEE 39th Photovoltaic Specialists Conference (PVSC)*, 2013: 2664-2668. <https://doi.org/10.1109/PVSC.2013.6745021>
- [8] HASHMI G., AKAND A.R., HOQ M., RAHMAN H., *Study of the enhancement of the efficiency of the monocrystalline silicon solar cell by optimizing effective parameters using PC1D simulation*, Silicon **10**(4), 2018: 1653-1660. <https://doi.org/10.1007/s12633-017-9649-3>
- [9] THIRUNAVUKKARASU G.S., SEYEDMAHMOUDIAN M., CHANDRAN J., STOJCEVSKI A., SUBRAMANIAN M., MARNADU R., ALFAIFY S., SHKIR M., *Optimization of mono-crystalline silicon solar cell devices using PC1D simulation*, Energies **14**(16), 2021: 4986. <https://doi.org/10.3390/en14164986>
- [10] AHMED M.S., AHMAD S.M., SUBHYALJADER M., *Study the role of effective parameters in enhancement of the silicon solar cell performance using PC1D simulation*, Journal of Ovonic Research **16**(2), 2020: 97-106.
- [11] GOETZBERGER A., KNOBLOCH J., VOSS B., *Crystalline Silicon Solar Cells*, Vol. 1., John Wiley & Sons, 1998. <https://doi.org/10.1002/9781119033769>
- [12] RAINA G., SINHA S., *A simulation study to evaluate and compare monofacial Vs bifacial PERC PV cells and the effect of albedo on bifacial performance*, Materials Today: Proceedings **46**, 2021: 5242-5247. <https://doi.org/10.1016/j.matpr.2020.08.632>
- [13] SEPEAI S., SULAIMAN M.Y., ZAIDI S.H., SOPIAN K., *Enhanced light absorption in bifacial solar cells*, [In] *2012 10th IEEE International Conference on Semiconductor Electronics (ICSE)*, 2012: 38-41. <https://doi.org/10.1109/SMElec.2012.6417086>
- [14] LEWIS M.R., TONITA E.M., VALDIVIA C.E., OBHI R.J.K., LESLIE J., BERTONI M.I., HINZER K., *Angular*



- dependence of textured bifacial silicon heterojunction solar cells for high latitudes*, [In] *2019 IEEE 46th Photovoltaic Specialists Conference (PVSC)*, 2019: 1919-1923. <https://doi.org/10.1109/PVSC40753.2019.8980857>
- [15] HAUG H., GREULICH J., *PC1Dmod 6.2 – Improved simulation of c-Si devices with updates on device physics and user interface*, *Energy Procedia* **92**, 2016: 60-68. <https://doi.org/10.1016/j.egypro.2016.07.010>
- [16] BASORE P.A., *Numerical modeling of textured silicon solar cells using PC-1D*, *IEEE Transactions on Electron Devices* **37**(2), 1990: 337-343. <https://doi.org/10.1109/16.46362>
- [17] PAN A.C., DEL CANIZO C., LUQUE A., *Effect of thickness on bifacial silicon solar cells*, [In] *2007 Spanish Conference on Electron Devices*, 2007: 234-237. <https://doi.org/10.1109/SCED.2007.384035>
- [18] BELARBI M., BENYUCEF A., BENYUCEF B., *Simulation of the solar cells with PC1D – Application to cells based on silicon*, *Advanced Energy: An International Journal (AEIJ)* **1**(3), 2014: 1-10.
- [19] VASOYA N.H., DHARMENDRA R., MODI K.B., *Effect of doping and thickness of si on superlative photovoltaic cell using PC1D*, *Global Research and Development Journal For Engineering* **5**(9), 2020: 1-6.
- [20] JANSSEN G.J.M., TOOL K.C.J., KOSSEN E.J., VAN AKEN B.B., CARR A.J., ROMIJN I.G., *Aspects of bifacial cell efficiency*, *Energy Procedia* **124**, 2017: 76-83. <https://doi.org/10.1016/j.egypro.2017.09.334>
- [21] PENG Z.-W., KODUVELIKULATHU L.J., KOPECEK R., *The impact of bulk resistivity on bifacial n-PERT rear junction solar cells*, [In] *2020 47th IEEE Photovoltaic Specialists Conference (PVSC)*, 2020: 1606-1610. <https://doi.org/10.1109/PVSC45281.2020.9301030>
- [22] EDLER A., MIHAILETCHI V.D., KODUVELIKULATHU L.J., COMPAROTTO C., KOPECEK R., HARNEY R., *Metallization-induced recombination losses of bifacial silicon solar cells*, *Progress in Photovoltaics* **23**(5), 2015: 620-627. <https://doi.org/10.1002/ppp.2479>
- [23] SUBRAMANIAN M., NAGARAJAN B., RAVICHANDRAN A., SUBHASH BETAGERI V., THIRUNAVUKKARASU G.S., JAMEI E., SEYEDMAHMOUDIAN M., STOJCEVSKI A., MEKHILEF S., MINNAM REDDY V.R., *Optimization of effective doping concentration of emitter for ideal c-Si solar cell device with PC 1 D simulation*, *Crystals* **12**(2), 2022: 244. <https://doi.org/10.3390/cryst12020244>

*Received May 2, 2021  
in revised form November 26, 2022*